# First Measurement of Prenucleation Molecular Clusters

**F. L. Eisele† and D. R. Hanson***

*Atmospheric Chemistry Division, NCAR, Boulder, Colorado 80307*

*Received: August 27, 1999; In Final Form: November 11, 1999*

The molecular cluster ions $HSO_4^-(H_2SO_4)_{n-1}$ corresponding to the neutral species $(H_2SO_4)_n$ for $n = 3-8$ have been observed using a transverse chemical ionization scheme located inside a cooled flow tube. The contribution of ion−molecule clustering reactions was ascertained and readily separated from the ionization of the neutral clusters. The presence of the clusters was strongly dependent on temperature and humidity. Ratios of successive clusters thought to be representative of steady-state are reported.

## Introduction

There is a growing interest in atmospheric aerosols because of the large uncertainties in their influence on global radiative forcing, their potential health hazards in urban and industrial areas, and their largely unexplored role in tropospheric chemistry. Even the source terms for their production are not well understood. In general, particles enter the atmosphere in three ways: they are swept up off land or ocean surfaces, they are formed by gas-to-particle nucleation processes, or they are injected into the atmosphere via volcanoes and combustion processes (natural and anthropogenic). The first of these processes is largely controlled by nature but is influenced by humans through changing land use. The gas-to-particle nucleation process occurs naturally, but it is highly nonlinear and is easily influenced by anthropogenic emissions of gases such as $SO_2$. The direct injection of particles into the atmosphere, from forest fires, for example, may involve a gas-to-particle nucleation process in the early stages. Aerosols that are injected into the atmosphere as a result of human activity often have their origin in some type of combustion process and are formed as a result of supersaturation/condensation of nonvolatile exhaust gases. Thus, an improved understanding of the rather elusive gas-to-particle nucleation process is central to quantifying both natural particle production and anticipated production increases in the rates resulting from human activity.

The important first steps to at least a portion of new particle formation events in the atmosphere likely involve the sulfuric acid molecule, $H_2SO_4$.[1] For example, two $H_2SO_4$ molecules may combine to give the $H_2SO_4$ dimer, another $H_2SO_4$ molecule may collide with the dimer resulting in a $H_2SO_4$ trimer, etc. The equilibrium constants for the successive addition of $H_2SO_4$ to these clusters

$$H_2SO_4 + H_2SO_4 \rightleftarrows (H_2SO_4)_2 \quad (1a)$$

$$H_2SO_4 + (H_2SO_4)_2 \rightleftarrows (H_2SO_4)_3 \quad (1b)$$

...

$$H_2SO_4 + (H_2SO_4)_{n-1} \rightleftarrows (H_2SO_4)_n \quad (1)$$

are $K_2$, $K_3$, ... $K_n$. There are other species in the atmosphere that may play a role in particle nucleation, notably $H_2O$ and $NH_3$.[2,3] Theoretical treatments based on bulk liquid properties (classical hydrate theory)[4,5] indicate that the hydration of $H_2SO_4$ and its clusters could be extensive. For example, at 50% relative humidity (RH), this theory predicts that the sulfuric acid monomer will be present primarily as $H_2SO_4 \cdot H_2O$ and $H_2SO_4 \cdot (H_2O)_2$. Therefore, reactions analogous to (1), including the hydration of (and possibly the addition of $NH_3$ to) the products and reactants, more suitably describe equilibrium when these species are present.

Attempts to explain particle formation in the atmosphere have been handicapped by insufficient thermodynamic information for reactions such as (1). In many regions of the atmosphere[1,2] and for some laboratory results,[6−8] the rate of particle formation is not adequately explained by binary homogeneous nucleation in the $H_2SO_4/H_2O$ system using thermodynamics derived from bulk solutions. The atmospheric inadequacies of the binary theories have led researchers to propose that $NH_3$ plays a role in particle formation,[2] and preliminary theory[3] and laboratory experiments[6] have demonstrated a pronounced effect on particle formation rates due to $NH_3$. Furthermore, in laboratory measurements of the reaction of $SO_3$ with $NH_3$, the dimer of sulfamic acid, $(NH_3SO_3)_2$, and its cluster with $H_2SO_4$, $NH_3SO_3H_2SO_4$, were observed.[9] This demonstrated a potential role that $NH_3$ may have in particle formation and also showed that clusters of this type can be investigated using CIMS.

This paper describes the measurement of molecular clusters of sulfuric acid under quiescent particle-growth conditions. It may be the first report of the detection of neutral $H_2SO_4$ clusters containing two to eight $H_2SO_4$ molecules, the large clusters being comparable to the critical cluster size found in laboratory experiments.[6] Although the measurements cover only a small range of concentration, the results provide a test for theory and reveal the power of the experimental technique. This technique provides a new window through which particle nucleation can be observed; each step of the process can now be studied. Finally, rough estimates of the steady-state ratios of successive clusters are derived from the measured ion-cluster distributions.

**Measurement and Analysis Techniques and Apparatus.** The measurement of $H_2SO_4$ and its clusters were made in a thermostated 9.5 cm i.d. flow tube using chemical ionization mass spectrometry (CIMS). The CIMS ion source and mass spectrometer inlet extend radially into the flow tube (3−6 and ~1 cm, respectively, from the wall) to detect species in situ. The ion−molecule reaction time was usually varied by changing

† Also School of Earth and Atmospheric Sciences, Georgia Institute of Technology, Atlanta, GA 30332.

10.1021/jp9930651 CCC: $19.00 
Published on Web 01/07/2000

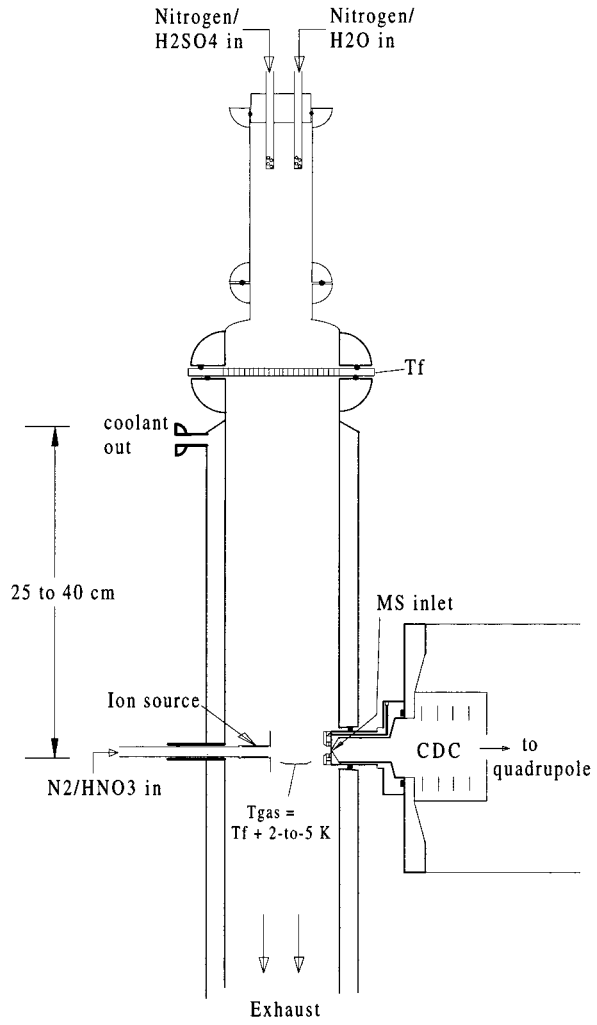


**Figure 1.** Schematic drawing of the cooled flow tube with the ion source and mass spectrometer inlet transverse to the flow. Ion reaction time is controlled by either changing the electric field or the distance between the source and the inlet.

the voltage applied to the ion-source; the distance between the source and the inlet could also be varied. A variable ion−molecule reaction time provided a means to distinguish between the ionization of neutral $H_2SO_4$ clusters and the ionization of ion−molecule clusters produced by the stepwise addition of $H_2SO_4$ molecules to $HSO_4^-$ ions. The $H_2SO_4$ concentration was kept low ($\sim 2 \times 10^9$ cm$^{-3}$) to minimize ion−molecule clustering while the flow tube temperature, $T_f$, was held at ∼240 K, to induce formation of neutral clusters of $H_2SO_4$.

A schematic of the apparatus is presented in Figure 1. Flows containing $H_2SO_4$ in $N_2$ and $H_2O$ in $N_2$ were mixed at 298 K and ∼620 Torr (slightly above local ambient pressure) in a 5 cm i.d. × 25 cm long region at the top of the flow tube. The $H_2SO_4$ and $H_2O$ sources are described in Ball et al.[6] At the end of an adaptor (5−9.5 cm i.d.) is located a cooled aluminum shower head assembly (0.64 cm thick with ∼150 holes 0.3 cm in diameter) that both collimates the flow and cools it to approximately $T_f$ + 12 K. Contact with the surfaces of the shower head results in about a factor of 2 loss of $H_2SO_4$. Once in the main flow tube (the temperature regulated section is ∼65 cm long and 255 K≤ $T_f$ ≤ 234 K), the gas mixture cools further to approximately 2−5 K over $T_f$ while it travels the 25−40 cm distance to the measurement region, at which the ion source and inlet are located. The total $N_2$ flow rate was 10−12 STP L min$^{-1}$ resulting in an average flow velocity of ∼2.5 cm s$^{-1}$; thus, a time period of 10−15 s was allowed for the gas to cool further and for $H_2SO_4$ to form clusters. $H_2SO_4$ and its clusters were ionized with $NO_3^-$ core reactant ions as they passed between the ion source and mass spectrometer inlet. The ions were prepared by flowing a dilute $HNO_3$-in-$N_2$ gas mixture through the ion source (a 0.64 cm i.d. × 2 cm long tube containing radioactive $^{241}$Am). The exit of the source is fitted with a 3 × 3 cm plate (0.2 mm thick) that has a 0.7 cm hole in the center through which the ions pass. The distance between the ion source and mass spectrometer entrance port (100 $\mu$m diameter hole) was generally 4 cm but was varied between 2.5 and 6 cm.

A collisional-dissociation chamber (CDC) is located just after the 100 $\mu$m entrance orifice, in which core ions can be stripped of associating species, such as $HNO_3$, before entering the differentially pumped mass spectrometer. In its typical application, the CDC is at a pressure of ∼0.1 Torr, and the application of an electric field of ∼10 V/cm will strip most of the ions of associating species.[10] Here, the electric field strength was kept low, ∼0.2−2 V/cm, enough to give an adequate transmission of ions through the CDC region but low enough to minimize the breakup of cluster ions. There was no evidence for the breakup of $HSO_4^-(H_2SO_4)_{n-1}$ clusters, as the CDC electric field was varied over this range. However, the amount of $HNO_3$ attached to the ions was observed to vary.

Ionization of $H_2SO_4$ occurs as the $NO_3^-$ and $(HNO_3)_mNO_3^-$ reactant ions (the majority of reactant ions are $m = 1$; hereafter, the reactant ions are referred to in short as $NO_3^-$ ions) traverse the central portion of the flow tube following the electric field lines which terminate at the entrance aperture to the mass spectrometer. The drift time of an ion is determined by its mobility, the electric field strength, and the distance it must travel. The ion source voltage was varied from −400 to −5000 V, resulting in drift times of ∼40−4 ms for a mobility of ∼1.5 cm$^2$/sV and a typical distance of 4 cm. This approximate drift time is the time for reaction of $NO_3^-$ with $H_2SO_4$ and with the $(H_2SO_4)_n$ molecular clusters under study. Also, during this time, $H_2SO_4$ vapor will cluster with the $HSO_4^-$ product ions (ion-induced cluster growth) leading to the identical ions as produced in the ionization of neutral clusters. Ion clusters such as $HSO_4^-(H_2SO_4)_n$ are strongly bound, and their rates of formation from $H_2SO_4$ + $HSO_4^-(H_2SO_4)_{n-1}$ are likely to be fast. It is assumed that both processes are contributing to the ions that are observed, and therefore, they are discussed in detail below.

The ion signals for the clusters were affected by mass discrimination within the instrument, notably the mass resolution of the quadrupole. For high-mass resolutions, such as a $\Delta m$ of ∼1 (fwhm) at 500 amu (see the inset in Figure 3), high-mass ions were suppressed; for example, the signal due to the hexamer was usually not observable. However, for low resolution settings, such as a $\Delta m$ of ∼10 at 500 amu (main part of Figure 3), many high mass ions were observed. For low resolution, the ratio of successive clusters was observed to be relatively insensitive to mass resolution for clusters up to $n = 6$. Figure 2 shows a plot of the ratios for the $n$th cluster/($n$ − 1)th cluster as a function of mass resolution setting. This setting primarily affects the mass resolution for mass peaks >150 amu ($\Delta m$ did not vary appreciably with mass below ∼100 amu.) Note that decreasing the resolution of the instrument may cause neighboring peaks to overlap/interfere with the ones in which we are interested, and this may be responsible for the variation in some of the ratios at low settings. Nonetheless, it is evident that most of the changes in these ratios occur at high mass resolutions; the

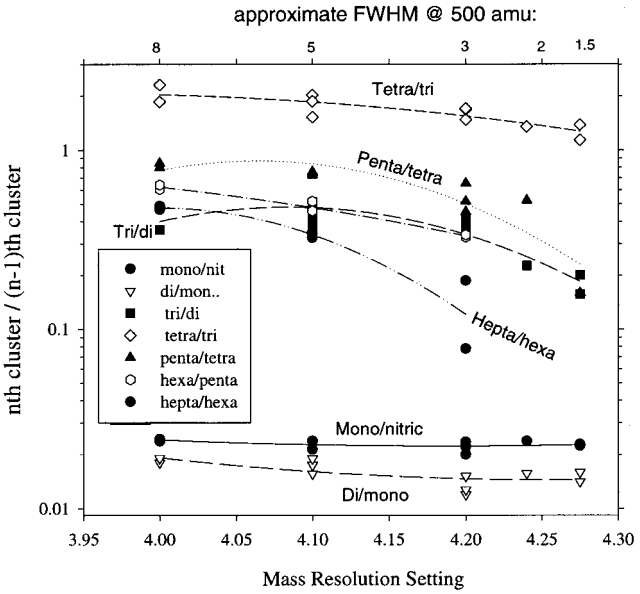


**Figure 2.** Ratios of successive clusters of $H_2SO_4$ vs mass resolution setting. The approximate fwhm of a mass peak at ~500 amu is indicated at the top of the figure.

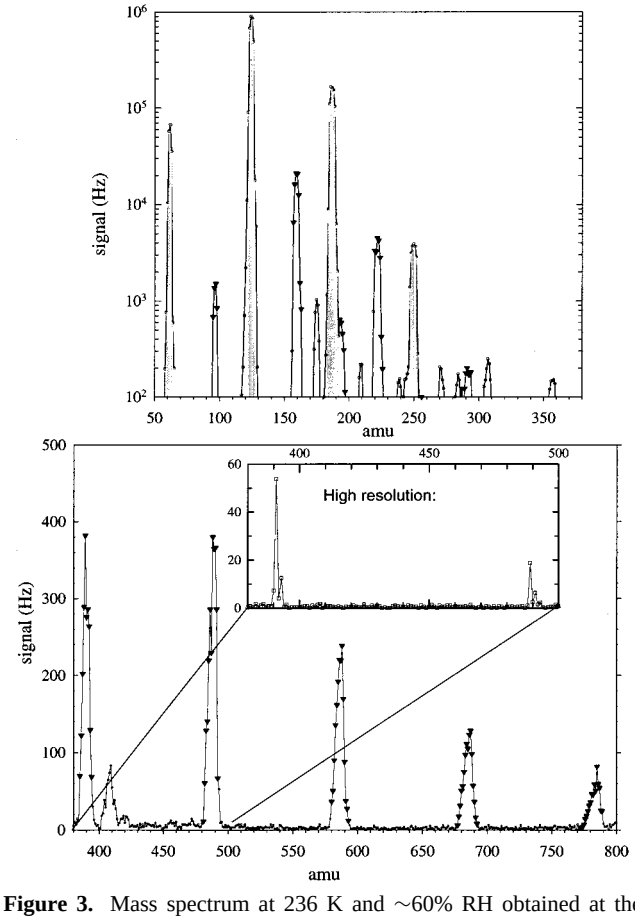


**Figure 3.** Mass spectrum at 236 K and ~60% RH obtained at the low-mass resolution used to calculate *Rn* values. The $[H_2SO_4]$ was ~1 × $10^9$ $cm^{-3}$. The $NO_3^-$ core ions are shaded in gray, and the ions associated with $H_2SO_4$ and its clusters are indicated by filled triangles. Note the change in logarithmic scale to linear scale at 380 amu. The inset is a higher resolution scan of the 391 and 489 amu peaks.

ratios of cluster signals are reported for low mass resolution (setting = 4.0) or corrected to these values using this plot. Other processes influencing mass discrimination, such as the lenses and detector/multiplier voltages, are likely to have only small effects on the ratios of successive clusters.

The temperature of the gas in the flow tube during these initial studies was not uniform, owing to the large cooling that must occur. The gas temperature a few cm from the flow tube wall was measured with a thermocouple probe. The aluminum shower head cooled the gas from 298 K to a temperature of $\sim T_f + 12$ K while it and the flow tube were at $T_f$. The gas cools to a temperature of $\sim T_f + 5$ K at a position of 25 cm into the flow tube (from the top) and to $T_{gas} \sim T_f + 2$ K after 40 cm of travel into the flow tube. These were the two positions of the ion detection region. The data presented here was generally taken at the 40 cm distance because of the longer residence time and the more uniform temperature (gradient, $\Delta T/\Delta z$, was ~0.3 K/cm whereas at 25 cm $\Delta T/\Delta z$ ~0.5 K/cm). However, comparisons with data from the 25 cm distance are also discussed. Despite the nonuniform temperature of the gas, the distributions determined from the signal ratios for some of the clusters could be representative of steady-state values.

How well the measurements reflect the steady-state distributions of the clusters is dependent on how fast each cluster equilibrates. If the forward rate coefficients for (1) are close to the collision rate and the dissociation rates are fast (comparable to or faster than the pseudo-first-order forward reaction rate coefficients), then our measurements may reflect steady-state or even equilibrium distributions. Results for the 25 and 40 cm distances (i.e., different neutral reaction times) are comparable and suggest that these assumptions are valid at least for the smaller clusters ($n = 2-4$). Determining equilibrium constants from the measured distributions requires a more stringent criterion; for example, the loss rate of the *n*th cluster to form the $(n + 1)$ cluster, due to addition of $H_2SO_4$, must be much less than the *n*th cluster's decomposition rate. If the *n*th cluster lies in the vicinity of the critical cluster, a dynamical model and accurate time information would be required to extract equilibrium constants.

**Ion Processes.** In the case of direct proton exchange between $NO_3^-$ and preexisting neutral clusters, the rates of ion formation are given by

$$NO_3^- + H_2SO_4 \rightarrow HSO_4^- + HNO_3 \quad (2)$$

for the monomer (which has a rate coefficient $k_1$) and for the *n*th cluster

$$NO_3^- + (H_2SO_4)_n \rightarrow HSO_4^-(H_2SO_4)_{n-1} + HNO_3 \quad (3)$$

with a rate coefficient, $k_n$. Thus, the incremental production of $HSO_4^-(H_2SO_4)_{n-1}$ in time d*t* from neutral cluster $(H_2SO_4)_n$, is approximately equal to

$$[NO_3^-][(H_2SO_4)_n]k_n dt \quad (4)$$

If it can be assumed that only small decreases in $[NO_3^-]$ occur by all ion−molecule reactions, then d*t* can be replaced by *t*, the ion-drift time for $NO_3^-$. This is the case for the measurements reported here, in which the sum of all product ion signals, a good indication of the extent of depletion of the reactant ion, was only a few percent of $NO_3^-$ core ions (see Figure 3.)

In the case of successive $H_2SO_4$ incorporation onto the $HSO_4^-$ ions formed in (2), the following series of reactions may occur:

$$HSO_4^- + H_2SO_4 \rightarrow HSO_4^-(H_2SO_4) \quad (5a)$$

...

$$HSO_4^-(H_2SO_4)_{n-2} + H_2SO_4 \rightarrow HSO_4^-(H_2SO_4)_{n-1} \quad (5n)$$

The rate coefficient for (5a) is designated $k'_2$, and similarly, the rate coefficient for (5$n$) is designated $k'_n$. The instantaneous production rate at time $\tau$ of the cluster with $n$ sulfuric acid species in it is given by

$$[H_2SO_4][HSO_4^-(H_2SO_4)_{n-2}](\tau)k'_n d\tau \quad (6)$$

where $[X](\tau)$ indicates the concentration of X at time $\tau$. Likewise, the production rate for the $HSO_4^-(H_2SO_4)_{n-2}$ ion is given by

$$[H_2SO_4][HSO_4^-(H_2SO_4)_{n-3}](\tau)k'_{n-1} d\tau \quad (7)$$

Starting with (2) and successively integrating (over $\tau$) these up to the $n$th cluster, the concentration of the $n$th ion cluster due to successive addition of $H_2SO_4$ to $HSO_4^-$ is given by

$$[NO_3^-][H_2SO_4]^n k_1 k'_2 ... k'_n \frac{t^n}{n!} \quad (8)$$

We have assumed that the decreases in ion concentrations due to reaction with $H_2SO_4$ are small, that $[H_2SO_4]$ is constant, and that the mobility of the ion is independent of $n$. The first assumption is reasonable, as discussed above. For the purposes of this discussion, the latter two assumptions are adequate.[12] Note that the values of $k_n$ and $k'_n$ rate coefficients are likely to be similar and also close to the effective ion collision rate, that is, on the order of $10^{-9}$ cm$^3$ s$^{-1}$.

The chemistry detailed above has been presented in a simplified manner. In the flow tube apparatus, for example, the $NO_3^-$ and $HSO_4^-$ ions are present primarily as cluster ions with a single $HNO_3$ molecule. These ions, as well as $H_2SO_4$ itself,[4] may have $H_2O$ molecules clustered with them. Treating these species as if they had no $HNO_3$ and $H_2O$ molecules associated with them is acceptable, because most, if not all, of the reactant ion clusters probably undergo similar reaction with $H_2SO_4$ and its hydrates, as do the core ions (even the rate coefficients are similar).[10,11] There is no information on the effect of $HNO_3$ and $H_2O$ on reactions 3 and 5, and we assume that their rates are also unaffected by the presence of $HNO_3$ or $H_2O$. Finally, although ionization of $H_2SO_4$ clusters via $HSO_4^-$ ions is likely to have a rate coefficient comparable to (3), this process is not taken into account here because $[HSO_4^-]$ is only a few percent of $[NO_3^-]$.

The principal difference between these two schemes, ionization of a preexisting neutral cluster versus product ion clustering with $H_2SO_4$, is their dependence on time. The production of ions from the $(H_2SO_4)_n$ neutral clusters has a linear time dependence for all $n$; thus, the ratio of any two of the ions produced from neutral clusters would be independent of ion reaction time. On the other hand, the $HSO_4^-(H_2SO_4)_{n-1}$ product of ion-induced clustering depends on time to the $n$th power and the ratio of any two ion clusters would have a dependence on time equal to the difference in the number of $H_2SO_4$ molecules in the clusters. Therefore, the ion-drift time dependence of the signals can be used to distinguish between neutral clusters and ion-induced clusters. By going to short reaction times and low $[H_2SO_4]$, such that ion-induced clustering is suppressed, the observed ions can be attributed to the ionization of neutral clusters, particularly in the production of large clusters.

Further evidence for detection of neutral clusters can be obtained by calculating the expected signal levels due to ion-clustering processes and comparing them to the observed signals. For ions due solely to successive addition of $H_2SO_4$ to $HSO_4^-$, the ratio of the ion cluster containing, for example, five $H_2SO_4$ moieties to that containing one $H_2SO_4$ moiety is approximately given by $([H_2SO_4]tk_1)^4/5!$. For illustration, $t$ and $k'_n$ are assumed independent of $n$ (see ref 12). With $[H_2SO_4] = 3 \times 10^9$ cm$^{-3}$, an ion-drift time $t = 10$ ms, and $k'_n = 10^{-9}$ cm$^3$ s$^{-1}$, ion-cluster growth from (8) would give a value of $\sim 10^{-8}$ for this ratio. If the observations of this ratio are much larger than this, as our results are, it indicates a detection of the neutral cluster. Also, the forward rate coefficients for ion clustering reactions are relatively insensitive to temperature and the presence of water vapor. If the measurements show strong dependencies on these two parameters, this would also indicate the detection of neutral clusters as opposed to ion clustering.

**Neutral Clustering Processes.** In order for the levels of neutral molecular clusters to be high enough to detect, there must be sufficient time available for these clusters to form in the flow tube. As mentioned above, this time is $\sim 10$ s (depending upon how cold the gas must be) or about $1 \times 10^3$ longer in duration than the ion−molecule reaction time. These neutral clusters are formed through a sequence of reactions as depicted above in (1). Analogous to the sequential ion clustering scheme, in which it is assumed that $[H_2SO_4]$ is constant over time $t$, that any cluster formed is not significantly depleted by the formation of a larger cluster, and that there is negligible decomposition of the clusters, the concentration of $(H_2SO_4)_n$ can be taken to be equal to $[H_2SO_4]^n t^{n-1} k_{2f} k_{3f} ... k_{nf}/(n-1)!$ where $k_{2f}$... $k_{nf}$ are the forward rate coefficients for (1a) to (1$n$), respectively. This is undoubtedly a simplification of the neutral system, the last assumption being particularly objectionable; however, this discussion is only for illustrative purposes. Again, using the example of the ratio of clusters containing five sulfuric acid molecules to those containing one sulfuric acid molecule and for $[H_2SO_4] = 3 \times 10^9$ cm$^{-3}$, $t = 0.7$ s, and $k_{nf} = 1 \times 10^{-10}$ cm$^3$ s$^{-1}$, a ratio of $\sim 10^{-4}$ for $[(H_2SO_4)_5]/[H_2SO_4]$ could be attained if unbridled coagulation occurs. This is clearly not a rigorous calculation, but it illustrates that if $H_2SO_4$ molecules react to form clusters at the gas-phase collision rate, which is a reasonable assumption, then a reaction time of as little as 1 s may be enough to allow for their presence at high enough levels to be observed (i.e., separated from ion-clustering processes).

## Results and Interpretation

Shown in Figure 3 is a mass spectrum taken at low resolution ($\Delta m \sim 10$ at 500 amu) with an ion-reaction time of $\sim 25$ ms, 0.12 Torr of water vapor, and a gas temperature of $-37$ °C (236 K). Masses associated with the initial core reactant ion, $NO_3^-$, are shaded in gray and are typically present as $NO_3^-$ (62 amu), nitric acid clusters $NO_3^-\cdot HNO_3$ (125 amu), and $NO_3^-\cdot(HNO_3)_2$ (188 amu). Ions that are associated with sulfuric acid are indicated by filled triangles. Individual sulfuric acid molecules are observed as $HSO_4^-$ (97 amu), $HSO_4^-\cdot HNO_3$ (160 amu), and $HSO_4^-\cdot(HNO_3)_2$ (223 amu) while the first sulfuric acid cluster is measured as the sum of $HSO_4^-\cdot H_2SO_4$ (195 amu) and $HSO_4^-\cdot H_2SO_4\cdot HNO_3$ (258 amu). Successive sulfuric clusters $(H_2SO_4)_n$ are observed as $HSO_4^-\cdot(H_2SO_4)_{n-1}$ (293, 391, 489, 587, 685, and 783 amu). Sulfuric clusters of three or more were not generally observed to cluster with $HNO_3$ (<1 Hz net signal). A high-resolution scan is included in the inset (Figure 3) to show the 34−32 sulfur isotopes for the 391 and 489 peaks. They were in the proper ratios and therefore helped to confirm the sulfate ion cluster peaks.[13] Note the absence of detection of any clusters containing $H_2O$ molecules.

The lack of observed $H_2O$ clustering on the nitric and sulfuric acid ions is probably due to a rapid loss of $H_2O$ molecules from the ions. Firstly, the ions may retain less water than the neutrals.

Secondly, any $H_2O$ associated with an ion may be driven off as the ion is sampled through the CDC (held at ~0.1 Torr $N_2$ and field strength of ~0.2 V/cm.) Water is far more volatile than sulfuric acid, and it likely reequilibrates with clusters much more quickly than does $H_2SO_4$ (i.e., fast rates for loss of $H_2O$.) Furthermore, the $H_2SO_4$ ion cluster distribution did not vary with the applied field in the CDC up to field strengths of a few V/cm. Thus, $H_2O$, but probably not $H_2SO_4$, can be lost during the ion's brief transit through this dry $N_2$ gas. Thus, although the effects of $H_2O$ on sulfuric acid cluster growth could be studied, the equilibrium water content of the clusters could not be directly observed.

As mentioned, $NO_3^-$ denotes the sum of $NO_3^-$ core ions (i.e., $NO_3^-$ + the nitric acid clusters listed above.) Also, we use the terminology monomers, dimers, trimers, and so forth to refer to the total number of sulfuric acid molecules plus $HSO_4^-$ core ions contained in an observed ion cluster, irrespective of the presence of $HNO_3$ molecules. Because $NO_3^-$ and its first two nitric acid clusters all react with $H_2SO_4$ at an ion collision rate of approximately $2 \times 10^{-9}$ cm$^3$/s at 298 K,[10,11] a rough estimate of $H_2SO_4$ concentration can be obtained from $(1/k_1t)ln([HSO_4^-]/[NO_3^-] + 1) \cong (1/k_1t)[HSO_4^-]/[NO_3^-]$ where the bracketed quantities are the signals for those ions. We use a value of $1.5 \times 10^{-9}$ cm$^3$ s$^{-1}$ for $k_1$ at the measurement temperature of ~240 K. It is not known how the $NO_3^-$ clusters react with the neutral sulfuric acid clusters, and we assume that the clusters are ionized with equal efficiency.[11]

Figure 4a shows a plot of $ln([HSO_4^-]/[NO_3^-] + 1)$ as a function of ion-drift time for water partial pressures of 0.12 and 0.04 Torr at ~236 K. Ion-drift time was set by varying the voltage on the ion source while maintaining a constant source-inlet distance of 4 cm. Because the ordinate should be equal to $k_1t[H_2SO_4]$, a linear time dependence is expected and $[H_2SO_4]$ is estimated to be $(1.2-2.4) \times 10^9$ molecule cm$^{-3}$, respectively. Linear regressions are also shown (Figure 4), and a nonzero intercept is exhibited. This is probably due to the fact that the field lines are not parallel because there are no guard rings in the flow tube and the sampling of ions and/or the ion−molecule reaction time may vary with the applied potential due to space-charge or other effects. It is also possible that $H_2SO_4$ is not evenly distributed in the gas, and thus, different amounts of $H_2SO_4$ could be sampled along the field lines.

The ion−molecule reaction time was also varied by changing the source-inlet gap, and the results for $[H_2SO_4]$ for the high RH conditions are shown in Figure 4a as the shaded triangles. The gap distance was varied from 2.5 to 5.7 cm while maintaining a constant electric-field strength. These results are in good agreement with the high RH data discussed above and bolster our confidence in the reliability of the calculated ion−molecule reaction time. Also, the signals for the $n = 2$ to 5 clusters were similar to those presented below obtained by varying the electric field strength. It is evident, however, that when the distance exceeds ~5 cm, the estimation of $[H_2SO_4]$ becomes increasingly inaccurate. This could be due to the gap becoming much greater than the sizes of the ion source exit plate (~3 cm) and the inlet face plate (~2 cm), thus allowing for increasingly divergent electric field lines.

The $[H_2SO_4]$ data for gaps of 4 cm and less can be used as a rough indication of the radial distribution of $[H_2SO_4]$, assuming the electric field does not change with gap distance. For example, $[H_2SO_4]$ near to the CIMS inlet (i.e., the data for source-inlet gaps of 2.5−3 cm) appears to be ~25% less than the $[H_2SO_4]$ measurement that spans the center of the tube (a 4 cm source-inlet gap). This indicates that $[H_2SO_4]$ is somewhat larger in the center of the flow tube, which is consistent with a loss of $H_2SO_4$ at the wall.

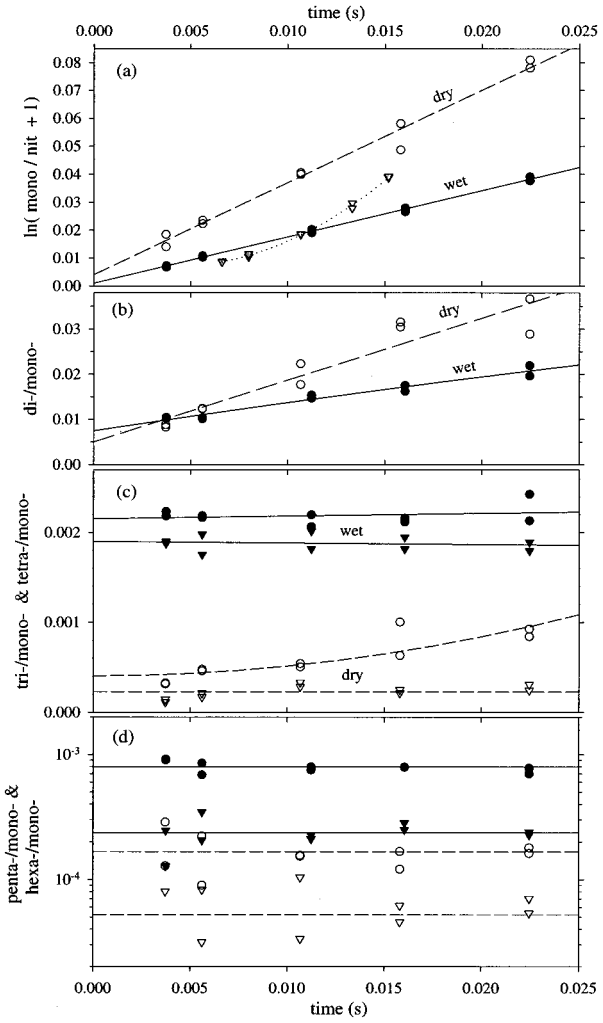


**Figure 4.** Ion ratios vs ion−molecule reaction time for two experiments at 236 K with water vapor at 0.12 Torr (filled symbols, solid lines) and 0.04 Torr (open symbols, dashed lines). (a) The monomer-to-nitric ratios are shown along with an experiment at the high RH where the source-inlet distance was changed (shaded triangles), (b) the dimer to monomer signal ratios, (c) the trimer and tetramer-to-monomer ratios, and (d) the pentamer and hexamer-to-monomer ratios are plotted on a log axis vs time.

Figure 4b−d shows the ratios of successive ion clusters of $H_2SO_4$ to that of the monomer. From the previous section, a time dependence is expected for any such ratio if the ion cluster is due to successive $H_2SO_4$ monomer addition to $HSO_4^-$ ions, and this is clearly exhibited for the dimer (linear) and for the trimer (quadratic) when the relative humidity is low, ~20% RH.[14] On the other hand, the ion clusters derived from a proton exchange between $NO_3^-$ and a preexisting neutral cluster should be time independent, and this is clearly evident for the $HSO_4^-(H_2SO_4)_{n-1}$ clusters for $n \geq 3$ at 63% RH and for $n \geq 4$ at 20% RH. Further evidence for the detection of the neutral clusters is exhibited in the magnitudes of the signals for the trimer and higher clusters at high RH versus those at low RH. The signals at low RH can be taken to be an upper limit to the effect of ion-induced clustering at high RH (indeed $[H_2SO_4]$ is lower at high RH), assuming there is no water dependence for this process. Thus, the observed signals cannot be due to ion clustering processes and are instead attributed to the presence of the neutral clusters $(H_2SO_4)_3$, $(H_2SO_4)_4$, and $(H_2SO_4)_5$.

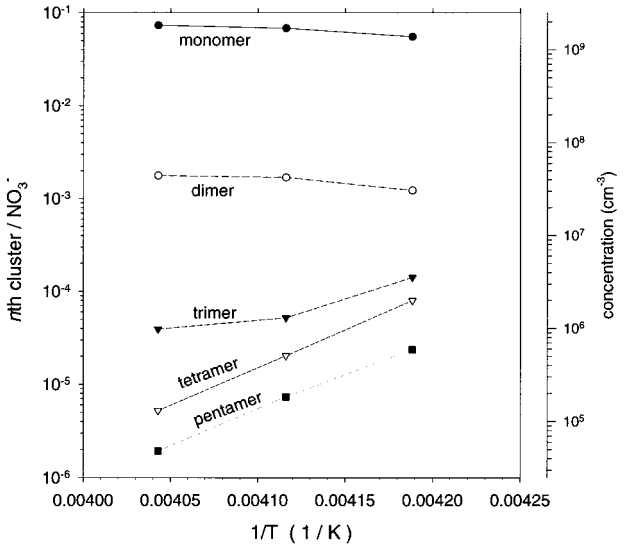


**Figure 5.** The $HSO_4^-(H_2SO_4)_{n-1}$ cluster signals up to $n = 5$ divided by the $NO_3^-$ ion signals are shown as a function of inverse temperature at a constant water vapor of 0.1 Torr. Note the apparent stabilization of the large clusters at low temperatures.

The effect of temperature on the ion signals is shown in Figure 5, a semilogarithmic plot of $[HSO_4^-(H_2SO_4)_{n-1}]/[NO_3^-]$ versus $1/T$. The ion-drift time was ~27 ms, and water vapor was constant at ~0.1 Torr. A resolution of $\Delta m = \sim 1$ at 500 amu was set for the mass spectrometer. The signal due to the monomer is relatively constant as the temperature was lowered, and the dimer signal changed only slightly (increased losses of $H_2SO_4$ due to temperature dependent eddies in the flow may be responsible for these changes), while the signals due to the the $n = 4$ and 5 $H_2SO_4$ clusters show substantial increases.

If a signal is due only to the ionization of a preexisting neutral species, then the quantity plotted on the *Y*-axis (Figure 5) can be related to the concentration of the neutral species. To the right of the plot is an alternative *Y*-axis that indicates [neutral] assuming a rate coefficient of $1.5 \times 10^{-9}$ cm$^3$ s$^{-1}$, a reaction time of 27 ms and negligible mass discrimination. This axis probably does not apply to the dimer signal because it is primarily due to the ion-clustering reaction. Assuming a negligible contribution from the neutral dimer, the ratio of the dimer to the monomer signals of 0.025 results in a value for $k'_2$ of $1 \times 10^{-9}$ cm$^3$ s$^{-1}$ for $HSO_4^- + H_2SO_4$ using $[H_2SO_4] = 1.8 \times 10^9$ cm$^{-3}$ (the mobilities of $NO_3^-$ and $HSO_4^-$ are likely to be similar; thus, the 2! term in 8 is accurate for $n = 2$). This is a reasonable value and indicates that the dimer ion signal ($n = 2$) is primarily due to the ion molecule clustering reactions. Likewise, the trimer-to-dimer ion signal ratio at the warmest temperature is ~0.025, suggesting that the $n = 3$ ion signal at this temperature may be primarily due to ion clustering reactions with $k'_3 \approx k'_2$.[12] As the temperature was lowered, however, the $n = 3$ signal due to the trimer neutral cluster appears. The $n = 4$ and 5 cluster signals, which show strong temperature dependencies, are especially notable and are likely due to the increasing stability of the neutral clusters $(H_2SO_4)_4$ and $(H_2SO_4)_5$ as the temperature is lowered. Because of the mass resolution setting for this experiment ($\Delta m = 1$ at 500 amu), the high-mass ions are discriminated against with respect to $[NO_3^-]$ (on the order of factors of 3 and 9, respectively). Taking this into account, the concentration of the $n = 4$ and 5 clusters is on the order of $1 \times 10^6$ to $1 \times 10^7$ cm$^{-3}$ at the coldest temperature.

The ratio of $(H_2SO_4)_5$ to $(H_2SO_4)_4$ decreases slightly as the temperature is lowered, and this indicates that the $(H_2SO_4)_5$ cluster is that in equilibrium, at least at the lower temperatures. Assuming the addition of $H_2SO_4$ to the fourth cluster is exothermic by 10−15 kcal mol$^{-1}$, and that this does not change with RH, the equilibrium ratio should increase by a factor of 2−3 as the temperature is decreased (the slight decrease in $[H_2SO_4]$ was taken into account). This observation may indicate that the lifetime of the fifth cluster may be longer than the growth time at ~236 K (a few seconds). It also may indicate that growth out of this cluster to $n = 6$ is faster than its decomposition rate, and a steady-state may have been approached. If this is true, the critical cluster for these conditions is less than $n = 5$, perhaps $(H_2SO_4)_4$.

**TABLE 1: Estimated Neutral Cluster Ratios**

| *T* (K) | $[H_2SO_4]$ (cm$^{-3}$) | $pH_2O$ (torr) | RH | R2[a] | R3[b] | R4[c] | R5[d] | additional clusters |
|---|---|---|---|---|---|---|---|---|
| 236 | $1 \times 10^9$ | 0.11 | 55% | ~0.01 | 0.4 | ~1 | ~1 | R6−8 ≈ 0.5 |
| 236 | $1.2 \times 10^9$ | 0.12 | 63% | ~0.008 | 0.3 | 0.9 | 0.4 | R6 ≈ 0.5 |
| 236 | $2.4 \times 10^9$ | 0.04 | 20% | ~0.005 | 0.05 | 0.6 | 1 | R6 ≈ 0.4 |
| 257 | $7 \times 10^8$ | 0.64 | 48% | ~0.004 | 0.06 | 0.14 | ~3 | |

[a] Observed signal was largely due to ion molecule clustering. Thus, the value was obtained by extrapolation. [b] The signals for $n = 3$ are mostly due to neutral clusters. R3, however, has the highly uncertain neutral dimer signal in the denominator. [c] This may be close to the critical cluster for the high humidity (RH > 50%) data. [d] Either there was insufficient time for steady state to be achieved or $n = 5$ is near the critical cluster size. For example, the 257 K observed ratio is higher than that at lower temperatures. See text for discussion.

Other observations indicate that the $n = 5$ and higher clusters have not reached equilibrium or steady state at the low temperatures. Data taken at ~50% RH at 257 K indicate a higher pentamer-to-tetramer ratio than the low temperature (~240K) data, which indicates that equilibrium for the fifth cluster was not attained at ~240 K. Also, data taken for comparable conditions at the two different neutral growth times (i.e., 25 and 40 cm) indicate that the pentamer (and to a lesser extent the tetramer) signal was larger for longer times. Therefore, for this and larger clusters at $T \leq 243$ K, the time to achieve steady-state/equilibrium is likely comparable to the time that $T_{gas}$ is within a few K of $T_f$, that is, a few seconds. Note also that this time is comparable to the inverse of the pseudo-first-order rate constant for formation of the *n*th cluster from the $(n - 1)$th cluster (~0.2 s$^{-1}$), assuming $k_{nf} \sim 10^{-10}$ cm$^3$ s$^{-1}$.

Cluster distributions can be derived from the ratio of the ion signals due to the clusters. Because the ion signals for small clusters (notably, $n = 2$) were significantly affected by ion clustering processes, the ratios of the 195 and 293 amu signals to the monomer signal, such as shown in Figure 4b and c, were extrapolated to zero ion time to get cluster/monomer ratios. Table 1 shows the observed cluster ratios for the data shown in Figures 3 and 4 and the 257 K data mentioned above. The data shown in Figure 5 is not included because it was taken at high mass resolution (thus the larger clusters were not observed) and also because the ion-drift time was not varied. *Rn* indicates the ratio $(H_2SO_4)_n/(H_2SO_4)_{n-1}$. Note that the notation $(H_2SO_4)_n$ is shorthand for the summation of $(H_2SO_4)_n(H_2O)_m$ over *m*.

The ratios R6 and higher are ~0.5, which may indicate that they are determined by the ratios of the efficiency of incorporation of $H_2SO_4$ into the successive clusters if steady-state had been attained. Then, for example, R6 $\approx k_{6f}/k_{7f}$ at steady state if the decomposition rate, $k_{6r}$, is very small. The measured ratios are consistent with an increase in $k_{nf}$ with *n* due to the increase in size of the cluster with *n*.

It is possible that for some clusters, that is, $n = 3$ and perhaps 4, the measurements reflect equilibrium distributions and thus $K_3$ or $K_4$ could be estimated. As mentioned above, the

appropriate equilibrium constants include the hydration of reactants and products whereas our measured ratios are likely to be the sum of all hydrated clusters. Thus in comparisons of theory with these results, the predicted equilibrium constants would need to be summed over all of the hydrates.

Our results are in accord with one theory of bimolecular nucleation, in which the critical cluster size is predicted to be $n \approx 4$ for these conditions.[15] In addition, this parametrization predicts that the nucleation rate is $1 \times 10^6$ to $1 \times 10^8$ particles $cm^{-3}$ $s^{-1}$ for the 50% RH conditions. Taking our observed concentration of the presumed critical cluster, $n = 4$, $\sim 1 \times 10^7$ $cm^{-3}$, and multiplying it by the first-order rate coefficient for the addition of an $H_2SO_4$ molecule, $[H_2SO_4]k_{5f}$, we arrive at an estimate of a few times $10^6$ particles $cm^{-3}$ $s^{-1}$ for the nucleation rate. For these types of theories and experiments, this agreement is remarkably quantitative.

## Conclusions

The present investigation provides new insight into the formation of molecular clusters of sulfuric acid and water. The experiments were done under temperatures and water concentrations that are typical of the middle-to-upper troposphere and the high latitude, lower troposphere. Unavoidably, the sulfuric acid concentrations were 1−2 orders of magnitude higher than those typical of the atmosphere. The experimental technique must also be refined in order to provide better, more quantitative results. Thus, direct application to the atmosphere awaits future revision of the technique. These include better determination of the time allowed for cluster growth and the attainment of a more uniform gas temperature in the flow tube.

These laboratory measurements are used to derive rough steady-state ratios of $H_2SO_4$ clusters that may be compared to those predicted by theories. This may be the first empirical data set against which the first steps of bimolecular nucleation theory can be tested. The results of this initial study are qualitatively in agreement with bimolecular nucleation theories[4,15] in that both suggest a positive correlation between cluster growth and water and acid concentrations and are suggestive that the critical cluster is near $n = 4$ at 240 K. Furthermore, there is semiquantitative agreement between the nucleation rate estimated from our measurements and the predicted[15] nucleation rates. Note that this theory was also in good agreement with recently[6] measured nucleation rates at 295 K and RH = 8%; however, some disagreements between measurements and predicted nucleation rates still exist, notably the RH dependencies.

We also presented evidence that the largest clusters observed, the pentamer through octamer, are probably greater than the size of a critical nucleus under the temperature and relative humidity condition of the experiment.[6,15] Thus, in addition to the first steps of the nucleation process, some of the growth steps may now be observable.

Another important aspect of this report is the demonstration that the nonvolatile chemical details of cluster growth can be observed. Bimolecular nucleation may be responsible for only a portion of the nucleation process in the remote atmosphere,[1] and new particle formation in urban environments is probably very removed from the simple $H_2SO_4/H_2O$ system. If other species are thought to influence particle nucleation in the atmosphere, they could be investigated using this experimental technique. It is likely that molecular information during cluster growth is required if anthropogenically induced nucleation is to be understood. In addition to refining the technique, we hope to extend these studies to include other species such as ammonia which has been shown to lead to enhanced nucleation rates when added to $H_2SO_4/H_2O$ gas mixtures.[6]

**Acknowledgment.** We thank D. Voisin for help in various aspects of this work and J. Orlando for helpful comments. Conversations with E. R. Lovejoy and P. McMurry are gratefully acknowledged. This research was in part supported by NASA Grant No. NAG5-6383.

## References and Notes

(1) Weber, R. J.; McMurry, P. H.; Mauldin, R. L.; Tanner, D. J.; Eisele, F. L.; Clarke, A. D.; Kapustin, V. N. *Geophys. Res. Lett. 26*, **1999**, 307.

(2) Weber, R. J.; Marti, J. J.; McMurry, P. H.; Eisele, F. L.; Tanner, D. J.; Jefferson, A. *Chem. Eng. Commun.* **1996**, *157*, 53.

(3) Coffman, D. J.; Hegg, D. A. *J. Geophys. Res.* **1995**, *100*, 7147.

(4) Jaecker-Voirol, A.; Mirabel, P. *J. Phys. Chem.* **1988**, *92*, 3518.

(5) Laaksonen, A.; Talanquer, V.; Oxtoby, D. W. *Annu. Rev. Phys. Chem.* **1995**, *46*, 489.

(6) Ball, S. M.; Hanson, D. R.; Eisele, F. L.; McMurry, P. H. *J. Geophys. Res.* **1999**, *104*, 23709.

(7) Viisanen, Y.; Kulmala, M.; Laaksonen, A. *J. Chem. Phys.* **1997**, *107*, 920.

(8) Wyslouzil, B. E.; Seinfeld, J. H.; Flagan, R. C.; Okuyama, K. *J. Chem. Phys.* **1991**, *94*, 6842.

(9) Lovejoy, E. R.; Hanson, D. R. *J. Phys. Chem.* **1995**, *100*, 4459.

(10) Eisele, F. L.; Tanner, D. J. *J. Geophys. Res.* **1993**, *98*, 9001. Tanner, D. J.; Jefferson, A.; Eisele, F. L. *J. Geophys. Res.* **1997**, *102*, 6415.

(11) Viggiano, A. A.; Seeley, J. V.; Mundis, P. L.; Williamson, J. S.; Morris, R. A. *J. Phys. Chem.* **1997**, 101, 8275.

(12) It is likely that there were gradients in $[H_2SO_4]$ in the detection region (see discussion concerning Figure 4a). The $[H_2SO_4]$ in the middle of the tube is crudely estimated to be approximately 30% higher than the average $[H_2SO_4]$. Also, the ion mobility of the $HSO_4^-(H_2SO_4)_{n-1}$ cluster is likely to be a weak function of $n$, approximately the inverse square root, and thus, the ion-drift time likely increases as $\sim n^{1/2}$. However, it is balanced somewhat by a compensating change in $k'_n$ with $n$: the collision rate of an ion with $H_2SO_4$ decreases as the mass of the ion increases. These facts about $t$, $k'_n$, and potential gradients in $[H_2SO_4]$ should be kept in mind when extracting values for the ion−molecule rate coefficients from the data. Because these factors are relatively small, we believe (8) is an adequate approximation for illustrative purposes.

(13) Several peaks, attributable to impurities, can be identified in Figure 2. Species giving ions at 113, 134, and 209 amu, and their clusters with $HNO_3$ and $H_2SO_4$, were observed. Also, signals at ~308 and ~408 amu are noticeable. The signals due to these species were highly variable and did not noticeably affect the observations of the sulfuric acid clusters, with only a few exceptions (e.g., the $^{34}S$ isotope for the dimer at 197 amu is also the mass for the $134 \cdot HNO_3$ ion). The isotopic ratios of the species giving the 113 amu ion were measured and are consistent with the species $CF_3CO_2^-$, the ion produced from reaction of $NO_3^-$ with triflouroacetic acid.

(14) A rough value for the rate coefficient $k'_3$ can be derived from the data in Figure 4c, assuming the trimer signal is due only to ion clustering: $k_2' \approx 8 \times 10^{-10}$. Note that the data follow a $t^2$ behavior.

(15) Kulmala, M.; Laaksonen, A.; Pirjola, L. *J. Geophys. Res.* **1998**, *103*, 8301.